Carbohydrate–Minor Groove Interactions in the Binding of Calicheamicin γ_1^I to Duplex DNA

Tianhu Li,† Zijian Zeng,† Virginia A. Estevez,† Kai U. Baldenius,† K. C. Nicolaou,*,‡ and Gerald F. Joyce*,§

Contribution from the Departments of Chemistry and Molecular Biology, The Scripps Research Institute, La Jolla, California 92037, and Department of Chemistry, University of California, San Diego, La Jolla, California 92093

Received January 3, 1994®

Abstract: The sequence-specific DNA cleavage activity of calicheamicin γ_1^I was studied using a synthetic 20mer DNA substrate that contains a single TCCT·AGGA target site. The cleavage reaction was initiated by addition of β-mercaptoethanol, which, under conditions of calicheamicin excess, results in burst kinetics. The burst amplitude was used to obtain a K_D value of 135 nM for the calicheamicin–DNA interaction. Calicheamicin and calicheamicin oligosaccharide were allowed to compete for binding, which provided a K_I value of 4.1 μM for the oligosaccharide–DNA interaction. Replacement of the iodo-substituted oligosaccharide by the corresponding bromo-, chloro-, fluoro-, methyl-, and hydrogen-substituted compounds resulted in progressively weaker binding. Replacement of guanine by inosine at the 5′-most but not the 3′-most position within the AGGA target sequence resulted in greatly diminished DNA cleavage. These results suggest that for this target sequence there is a critical interaction between the iodine substituent on the calicheamicin oligosaccharide and the 5′-most guanine C2-NH_2 group within the minor groove of the target DNA.

Introduction

The enediyne antitumor antibiotics, including calicheamicin γ_1^I (**1**) and esperamicin A_1, bind to the minor groove of duplex DNA in a sequence-specific manner.[1-3] In the case of cali-

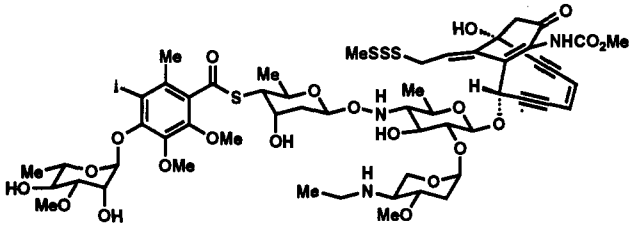

1: calicheamicin γ_1^I

cheamicin, binding occurs along short runs of oligopyrimidine·oligopurine base pairs, such as TCCT·AGGA.[1,2,4,5] Once bound, calicheamicin promotes cleavage of both strands of the DNA through a remarkable free-radical mechanism that involves a Bergman-type cycloaromatization to generate a reactive diradical species[4,6,7] (Scheme 1). The two strands of the DNA

Scheme 1

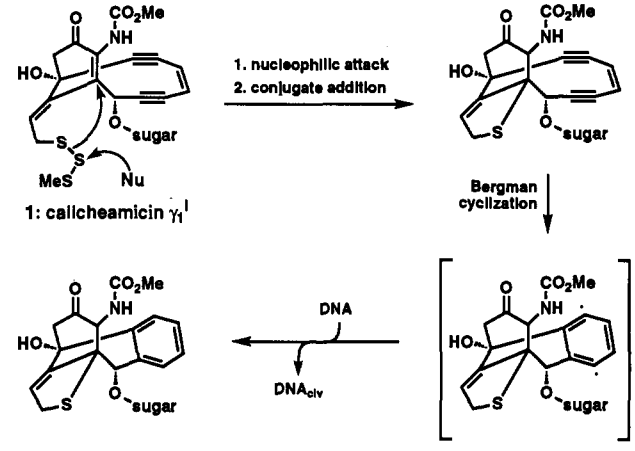

1: calicheamicin γ_1^I

are cleaved in a concerted fashion following abstraction of a C5′ hydrogen from the oligopyrimidine strand and a C4′ hydrogen from the oligopurine strand.[4,7] The cycloaromatization reaction and subsequent DNA cleavage are triggered by reduction of the trisulfide moiety that is attached to the enediyne ring. In the absence of a reductant, calicheamicin binds to the DNA but does not promote strand cleavage.

Previous studies have shown that calicheamicin binds to the target sequence with high affinity. The dissociation constant, K_D, for binding of calicheamicin to duplex DNA has been estimated to be on the order of 10^{-8} M for TCCT·AGGA sites[5] and 10^{-6} M for a mixture of sites within pBR322 DNA.[8] Most but not all of the binding energy is thought to derive from interactions involving the carbohydrate domain of calicheamicin within the minor groove of the DNA. Calicheamicinone, which lacks the carbohydrate domain, binds to DNA with low affinity and in a non-sequence-specific manner.[5] In contrast, the

† Department of Chemistry, The Scripps Research Institute.
‡ Department of Chemistry, The Scripps Research Institute, and Department of Chemistry, University of California, San Diego.
§ Departments of Chemistry and Molecular Biology, The Scripps Research Institute.

® Abstract published in *Advance ACS Abstracts,* March 15, 1994.

(1) Zein, N.; Sinha, A. M.; Megahren, W. J.; Ellestad, G. A. *Science* **1988**, *240*, 1198–1201.
(2) Zein, N.; Poncin, M.; Nilakantan, R.; Ellestad, G. A. *Science* **1989**, *244*, 697–699.
(3) (a) Long, B. H.; Golik, J.; Forenza, S.; Ward, B.; Rehfuss, R.; Dabrowiak, J. C.; Catino, J. J.; Musial, S. T.; Brookshire, K. W.; Doyle, T. W. *Proc. Natl. Acad. Sci. U.S.A.* **1989**, *86*, 2–6. (b) Sugiura, Y.; Uesawa, Y.; Takahashi, Y.; Kuwahara, J.; Golik, J.; Doyle, T. W. *Proc. Natl. Acad. Sci. U.S.A.* **1989**, *86*, 7672–7676. (c) Nicolaou, K. C.; Dai, W. M. *Angew. Chem.* **1991**, *30*, 1387–1416.
(4) Devoss, J. J.; Townsend, C. A.; Ding, W. D.; Morton, G. O.; Ellestad, G. A.; Zein, N.; Tabor, A. B.; Schreiber, S. L. *J. Am. Chem. Soc.* **1990**, *112*, 9669–9670.
(5) Drak, J.; Iwasawa, N.; Danishefsky, S.; Crothers, D. *Proc. Natl. Acad. Sci. U.S.A.* **1991**, *88*, 7464–7468.
(6) Ellestad, G. A.; Hamann, P. R.; Zein, N.; Morton, G. O.; Siegel, M. M.; Pastel, M.; Borders, D. B.; McGahren, W. J. *Tetrahedron Lett.* **1989**, *30*, 3033–3036.
(7) Hangeland, J. J.; De Voss, J. J.; Heath, J. A.; Townsend, C. A. *J. Am. Chem. Soc.* **1992**, *114*, 9200–9202.
(8) Ding, W.-D.; Ellestad, G. A. *J. Am. Chem. Soc.* **1991**, *113*, 6617–6620.

0002-7863/94/1516-3709$04.50/0

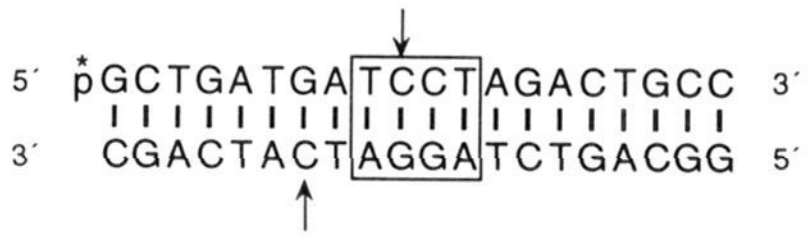

Figure 1. Synthetic 20mer duplex DNA containing a single TCCT·AGGA target site (boxed region) for recognitiion by calicheamicin. Arrows denote sites of calicheamicin-induced DNA cleavage. The TCCT-containing strand was [5′-^{32}P]-labeled (see Experimental Section).

carbohydrate domain alone exhibits much of the binding affinity and sequence specificity that is characteristic of the intact molecule.[9,10]

In the present study, we carried out a kinetic analysis to measure the binding affinity between calicheamicin and a single TCCT·AGGA site within a synthetic duplex DNA. We also carried out a competitive binding analysis involving both calicheamicin and the calicheamicin oligosaccharide (**2**), enabling us to measure the DNA binding affinity of the carbohydrate domain alone. Previously, we showed that the iodine substituent

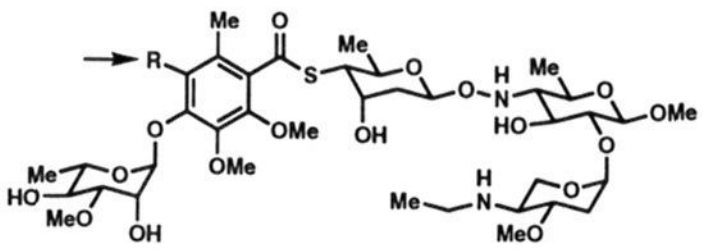

2: R = I **5**: R = F
3: R = Br **6**: R = CH_3
4: R = Cl **7**: R = H

on the aromatic C ring of the carbohydrate domain is critical for its ability to bind to certain DNAs in a sequence-specific manner.[10] This result prompted us to prepare a variety of analogues of the calicheamicin oligosaccharide (**3**–**7**) that differ with respect to the substituent at the position of iodination. We then measured the DNA binding affinity of each of these analogues. It has been suggested that the iodine moiety interacts with the exocyclic C2-NH_2 of both guanine residues that lie within the oligopurine strand of the target DNA.[11] Recent NMR data suggest that the iodine is in a position to interact with the first (5′-most) but not the second guanine C2-NH_2.[12] To evaluate this issue, we measured the binding affinity between calicheamicin and duplex DNA that contains either AGGA, AIGA, AGIA, or AIIA within the oligopurine region of the target DNA (I = inosine, lacking the C2 amine).

Results

Determination of the Calicheamicin–DNA Binding Constant. In order to simplify the kinetic analysis of the interaction between calicheamicin and a DNA target, we designed a 20mer duplex DNA that contains a single TCCT·AGGA site flanked by a total of 16 base pairs (Figure 1). The TCCT-containing strand was [5′-^{32}P]-labeled and hybridized with a 100-fold molar excess of the unlabeled AGGA-containing strand. Varying concentrations of calicheamicin, always in large excess over the duplex DNA, were added to the reaction mixture and allowed to equilibrate at 37 °C for 30 min in the absence of a reducing agent. β-Mercaptoethanol (30 mM final concentration) was added to trigger the cycloaromatization of calicheamicin, and samples were taken from the reaction mixture at frequent time intervals. The sampled material was analyzed by denaturing polyacrylamide gel electrophoresis, which allowed quantitation of both the cleaved and uncleaved DNA.

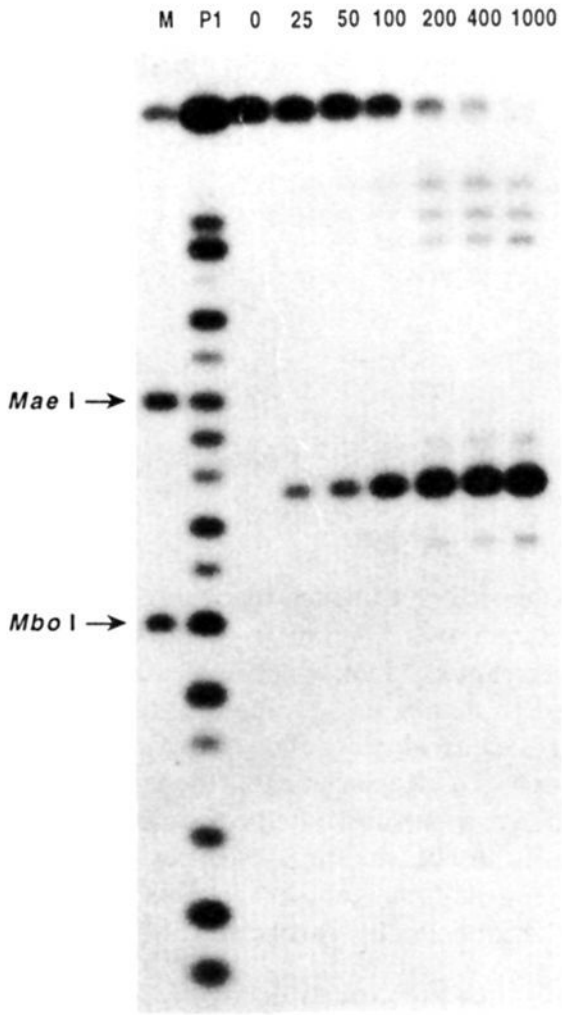

Figure 2. Autoradiogram of a denaturing polyacrylamide gel showing products of calicheamicin-induced DNA cleavage within the [5′-^{32}P]-labeled, TCCT-containing strand. M, marker lane containing an equimolar mixture of the products of DNA digestion with either *Mae*I (cleaves 5′-CŤAG) or *Mbo*I (cleaves 5′-ĞATC) restriction enzymes. P1, oligonucleotide ladder resulting from partial DNA digestion with P1 nuclease (generates 3′-OH terminus). 0–1000, products of DNA digestion in the presence of varying concentrations of calicheamicin γ_1^I, ranging from none to 1000 nM, following incubation at 37 °C for 6 min (see Experimental section). Calicheamicin-induced DNA cleavage generates a 3′-phosphate terminus, accounting for the slightly faster mobility of the labeled cleavage product compared to the P1 ladder.

As expected, cleavage of the target DNA occurs at a single, preferred site within the radiolabeled strand, corresponding to the 5′-most C residue within the TCCT sequence (Figure 2). At high concentrations of calicheamicin (≥200 nM), a small amount of nonspecific cleavage is observed both upstream and downstream from the preferred cleavage site. These nonspecific cleavage events contribute to the consumption of the DNA starting material but not to the yield of the expected product. Thus, estimates of the fraction cleaved (F_{clv}) that are based on the ratio of expected product to the sum of expected product plus unreacted starting material will be slightly overstated, especially at high concentrations of calicheamicin.

A simplified kinetic scheme for the reaction of calicheamicin with radiolabeled DNA considers the association rate (k_1) and dissociation rate (k_{-1}) of these two compounds and the rate of calicheamicin-induced DNA cleavage (k_2) (Scheme 2). During the time of preincubation prior to addition of the thiol, calicheamicin becomes equilibrated between the bound and unbound states, based on its total concentration relative to K_D. Addition of a large excess of β-mercaptoethanol results in the rapid activation of calicheamicin. The fate of the calicheamicin–DNA complex depends on the relative rates of complex dissociation versus calicheamicin-induced DNA cleavage. If $k_{-1} > k_2$, then the complex will tend to dissociate before DNA cleavage can occur, and the apparent rate of cleavage will reflect either the rate of association or the rate of the chemical step, whichever is

(9) Aiyar, J.; Danishefsky, S. J.; Crothers, D. M. *J. Am. Chem. Soc.* **1992**, *114*, 7552–7554.
(10) Nicolaou, K. C.; Tsay, S.-C.; Suzuki, T.; Joyce, G. F. *J. Am. Chem. Soc.* **1992**, *114*, 7555–7557.
(11) Hawley, R. C.; Kiessling, L. L.; Schreiber, S. L. *Proc. Natl. Acad. Sci. U.S.A.* **1989**, *86*, 1105–1109.
(12) Walker, S.; Murnick, J.; Kahne, D. *J. Am. Chem. Soc.* **1993**, *115*, 7954–7961.

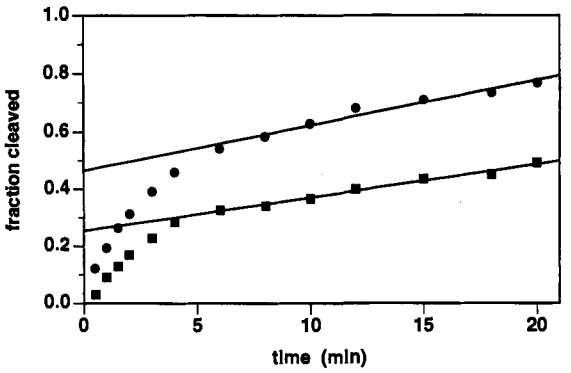

Figure 3. Time course of calichemicin-induced DNA cleavage following addition of β-mercaptoethanol (see Experimental Section). (■), 50 nM calicheamicin, ●, 100 nM calicheamicin. Linear regression analysis was used to fit a line to the data points from 6 to 20 min, the intercept providing an estimate of the burst amplitude.

Scheme 2

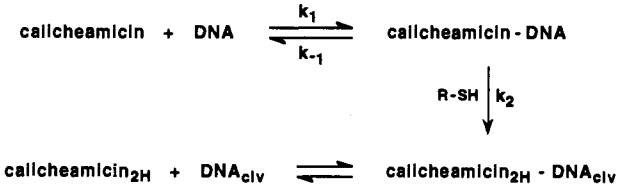

slower. If $k_{-1} < k_2$, then any DNA that is bound by calicheamicin will tend to undergo cleavage before dissociation can occur. In this case, one would expect to see an initial burst, reflecting the amount of DNA that is in the bound state at the time of thiol addition, followed by a slower phase resulting from subsequent association and cleavage events.

In a series of preliminary experiments, we found that the reaction indeed exhibits burst kinetics (Figure 3). There is an initial phase of rapid DNA cleavage, lasting only a few minutes, followed by a longer period of steady accumulation of the cleavage product. Extrapolating back from the linear phase of the reaction, one can determine the burst amplitude, expressed as the fraction of DNA cleaved at $t = 0$. The burst amplitude corresponds to the initial concentration of calicheamicin–DNA complex relative to the total amount of DNA and can be used to obtain an estimate of K_D.[13] The reaction products are analyzed on a denaturing polyacrylamide gel, so that dissociation of the reacted calicheamicin–DNA complex does not enter into the analysis. The reaction of calicheamicin with duplex DNA is irreversible, and reacted calicheamicin cannot be regenerated to carry out a second DNA cleavage reaction. Extending the preincubation time from 30 min to 1 h did not affect the burst amplitude, indicating that the binding of calicheamicin to DNA had reached equilibrium prior to addition of the thiol. Increasing the concentration of β-mercaptoethanol to 100 mM had no effect on the burst amplitude, demonstrating that the reaction is not limited by the availability of the thiol.

We carried out a series of time course experiments and determined the burst amplitude over a range of calicheamicin concentrations (12.5–400 nM). This allowed us to obtain a saturation profile for the interaction between calicheamicin and a single TCCT·AGGA site within duplex DNA (Figure 4). An estimate of K_D is provided by the calicheamicin concentration at the midpoint of the saturation curve, roughly 100 nM. However, the best-fit saturation curve has a slight positive deviation from an ideal binding curve, especially at high calicheamicin concentrations. We attribute this slight deviation to nonspecific cleavage

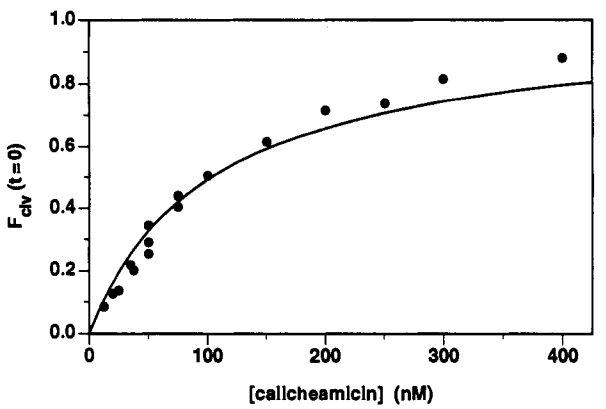

Figure 4. Burst amplitude (fraction cleaved at $t = 0$) of calicheamicin-induced DNA cleavage, determined at varying concentrations of calicheamicin. Data were fit by a least-squares method to a theoretical binding curve (indicated by solid line), given by the equation F_{clv} = [calicheamicin]/(K_D + [calicheamicin]).

events that occur more readily at high calicheamicin concentrations (see above). Extrapolating the calicheamicin–DNA binding data to very low calicheamicin concentration, we obtain a value for K_D of 135 ± 6 nM.[14]

Determination of Oligosaccharide–DNA Binding Constants. Knowing K_D for the calicheamicin–DNA interaction, it is possible to determine the inhibition constant, K_I, for binding of the calicheamicin oligosaccharide (**2**) in competition with intact calicheamicin at a single TCCT·AGGA site within duplex DNA. We assume that these two compounds are strict competitive inhibitors that bind to the target site in a mutually exclusive fashion. Following hybridization of the two strands of the DNA duplex, varying concentrations of calicheamicin and calicheamicin oligosaccharide were added to the reaction mixture, and the mixture was allowed to equilibrate at 37 °C. β-Mercaptoethanol was added, and samples were withdrawn at frequent intervals to monitor the time course of calicheamicin-dependent DNA cleavage. Burst kinetics were observed over a broad range of calicheamicin concentrations, with the burst amplitude being reduced depending on the concentration of the calicheamicin oligosaccharide.

During the preincubation period, the labeled DNA becomes distributed between three states: calicheamicin-bound, oligosaccharide-bound, and free, with only the first contributing to the burst upon addition of the thiol. We consider the following three equations, which apply to the binding equilibrium that is reached during the preincubation period:

$$[\text{calich–DNA}] = [\text{DNA}][\text{calich}]/K_D \quad (1.1)$$

$$[\text{oligosac–DNA}] = [\text{DNA}][\text{oligosac}]/K_I \quad (1.2)$$

$$[\text{DNA}_{total}] = [\text{DNA}] + [\text{calich–DNA}] + [\text{oligosac–DNA}] \quad (1.3)$$

From these equations, we derive an expression relating the burst amplitude, $F_{clv}(t = 0)$, to the concentrations of calicheamicin and calicheamicin oligosaccharide and their respective binding constants:

$$F_{clv} = [\text{calich–DNA}]/[\text{DNA}_{total}] \quad (2.1)$$

(13) $[\text{DNA}_{total}] = [\text{DNA}] + [\text{calich–DNA}]$; $[\text{calich–DNA}] = [\text{DNA}]\cdot[\text{calich}]/K_D = ([\text{DNA}_{total}] - [\text{calich–DNA}])[\text{calich}]/K_D$; $[\text{DNA}_{total}]/[\text{calich–DNA}] = 1 + (K_D/[\text{calich}])$; $F_{clv}(t = 0) = [\text{calich–DNA}]/[\text{DNA}_{total}] = [\text{calich}]/(K_D + [\text{calich}])$.

(14) $F_{clv}/[\text{calich}] = 1/(K_D + [\text{calich}])$. Thus a plot of $[\text{calich}]/F_{clv}$ versus [calich] is expected to give a straight line with slope 1 and intercept K_D. In fact, the plot is linear ($r = 0.98$), with a slope of 0.78 ± 0.04 and an intercept of 135 ± 6 nM.

$$F_{clv} = K_I[\text{calich}]/(K_I[\text{calich}] + K_D[\text{oligosac}] + K_IK_D) \quad (2.2)$$

$$[\text{calich}](1 - F_{clv})/F_{clv} = ([\text{oligosac}]K_D/K_I) + K_D \quad (2.3)$$

Thus, a plot of [calicheamicin]$(1 - F_{clv})/F_{clv}$ versus [oligosaccharide] is expected to give a straight line with slope K_D/K_I and intercept K_D. The value for K_D is already known and will be confirmed by the intercept determination. The value for K_I can be obtained from the slope if K_D is known.

The plot of [calicheamicin]$(1 - F_{clv})/F_{clv}$ versus [oligosaccharide], obtained at varying concentrations of calicheamicin oligosaccharide (0–20 μM) and two different concentrations of calicheamicin (5, 20 nM), is linear ($r = 0.99$), with an intercept of approximately 100 nM (Figure 5a). From the slope, we obtain a value for K_I of $4.1 \pm 0.4\,\mu$M. Thus, binding of the calicheamicin oligosaccharide to a TCCT·AGGA site within duplex DNA is about 30-fold weaker than binding of intact calicheamicin. This corresponds to a free energy difference (at 37 °C) of 2.1 kcal mol^{-1}.

A similar competitive binding analysis was carried out to determine the DNA binding affinity of a variety of analogues of the calicheamicin oligosaccharide (**3**–**7**) that differ at the position of iodine substitution on the aromatic C ring. These analogues include the bromo-, chloro-, fluoro-, methyl-, and hydrogen-substituted compounds. In each case, the plot of [calicheamicin]-$(1 - F_{clv})/F_{clv}$ versus [oligosaccharide] is linear ($r_{min} = 0.93$), with an intercept in the range 110–160 nM (Figure 5b–f). The DNA binding affinity of the various analogues declines in the order: iodo > bromo > chloro ≥ methyl ≥ fluoro ≫ hydrogen (Table 1). Replacement of iodine with hydrogen results in the loss of about 2.3 kcal mol^{-1} of binding energy.

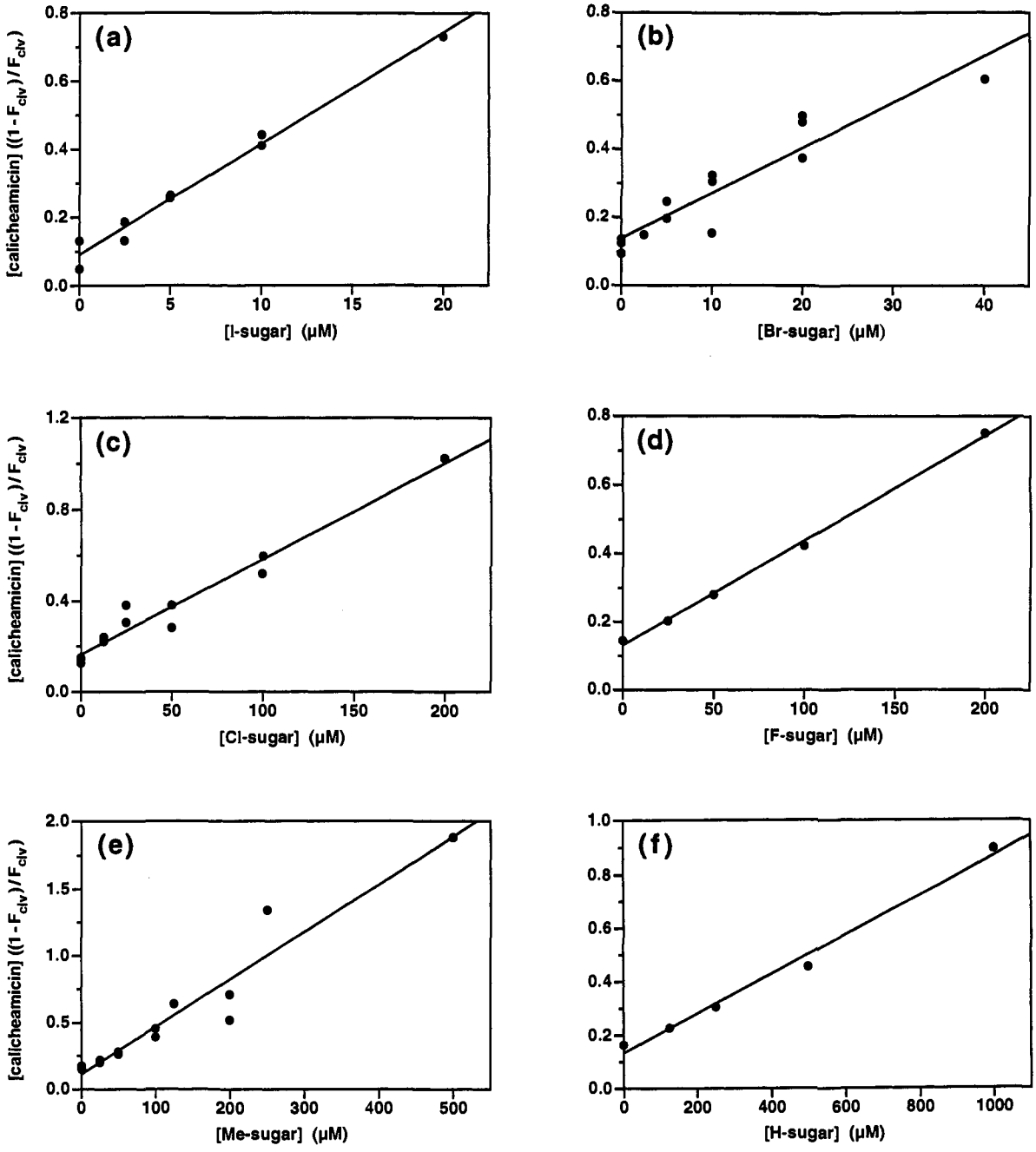

Figure 5. Plots of [calicheamicin]$(1 - F_{clv})/F_{clv}$ versus [oligosaccharide] used to determine K_I for various analogues of the calicheamicin oligosaccharide. (a) Compound **2**; (b) compound **3**; (c) compound **4**; (d) compound **5**; (e) compound **6**; and (f) compound **7**. Linear regression analysis was used to fit a line to each set of data points.

Table 1. Binding Affinity of Calicheamicin and Various Analogues of the Calicheamicin Oligosaccharide at a Single TCCT·AGGA Site within Duplex DNA

bound ligand	K_{obs}[a] (μM)	ΔG[b] (kcal mol^{-1})	$\Delta\Delta G$[c] (kcal mol^{-1})	r[d] (Å)
calicheamicin (**1**)	0.135 ± 0.006	–9.7		
I sugar (**2**)	4.1 ± 0.4	–7.6	2.1	2.15
Br sugar (**3**)	10.0 ± 1.7	–7.1	2.6	1.95
Cl sugar (**4**)	32.0 ± 3.3	–6.4	3.3	1.80
F sugar (**5**)	44.0 ± 3.1	–6.2	3.5	1.35
CH_3 sugar (**6**)	38.0 ± 5.0	–6.3	3.4	2.00
H sugar (**7**)	180.0 ± 19.0	–5.3	4.4	1.20

[a] K_{obs} is the apparent dissociation constant of either calicheamicin (K_D) or calicheamicin oligosaccharide (K_I), shown with the standard error. [b] $\Delta G = RT \ln K_{obs}$; $T = 310.15$ K, $R = 1.987$. [c] $\Delta\Delta G$ is ΔG for the oligosaccharide relative to ΔG for intact calicheamicin. [d] r is the van der Waals radius of the substituent on the C ring of the calicheamicin oligosaccharide.

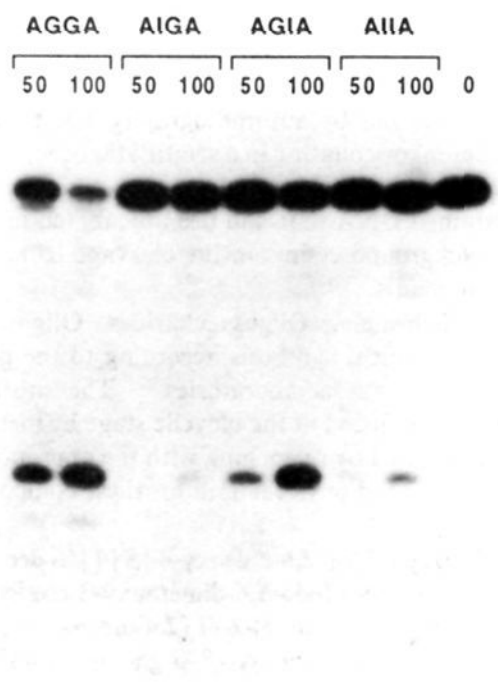

Figure 6. Autoradiogram of a denaturing polyacrylamide gel showing products of calicheamicin-induced DNA cleavage within the [5′-^{32}P]-labeled, TCCT-containing strand. The opposing strand contained either 5′-AGGA, 5′-AIGA, 5′-AGIA, or 5′-AIIA. The reaction was carried out at 37 °C for 10 min, employing either 50 or 100 nM calicheamicin.

Role of Guanine C2-NH_2 Groups in Oligosaccharide–DNA Binding. Binding of calicheamicin at a TCCT·AGGA site places the iodine substituent of the C ring in close proximity to one or both of the guanine C2-NH_2 groups within the minor groove of the duplex DNA.[11,12] We prepared analogues of the 20mer DNA duplex (Figure 1) that lack the C2-NH_2 group at either one or both of the target site guanine residues. This is accomplished by replacing guanine with inosine while maintaining the TCCT sequence in the opposing strand. Replacing the target 5′-AGGA by 5′-AIGA greatly diminishes calicheamicin binding and subsequent DNA cleavage (Figure 6). Replacing 5′-AGGA by 5′-AGIA, on the other hand, causes only a modest reduction of DNA binding affinity ($K_D \approx 300$ nM) and no change in the site specificity of the DNA cleavage reaction. Replacing 5′-AGGA by 5′-AIIA gives results similar to those obtained with 5′-AIGA. Thus the first (5′-most) but not the second guanine C2-NH_2 is important for tight binding of calicheamicin at a TCCT·AGGA site within duplex DNA.

Discussion

We were at first surprised to observe burst kinetics for calicheamicin-induced DNA cleavage upon addition of the thiol to a preequilibrated mixture of calicheamicin and duplex DNA. Townsend and colleagues have shown that the second-order rate constant for thiol-dependent activation of calicheamicin is on the order of 0.1 M^{-1} s^{-1},[15] while Kahne and colleagues have measured the rate constant for dissociation of a calicheamicin–DNA complex as 3 s^{-1}.[12] Thus, at 30 mM thiol concentration, as was employed in this study, one would expect the apparent rate of thiol activation and subsequent DNA cleavage to be slower than 0.01 s^{-1}. If this were true, then any calicheamicin–DNA complex that exists at the time of thiol addition would likely dissociate before DNA cleavage could occur, and there would be no initial burst. The fact that we do observe a burst, in a single-turnover reaction with calicheamicin in large excess over the labeled DNA, indicates that there is some preactivated complex that is more likely to undergo DNA cleavage than dissociation upon addition of the thiol. We interpret this preactivated complex as corresponding to calicheamicin bound at the TCCT·AGGA target site. This interpretation is consistent with the saturation profile obtained for calicheamicin alone (Figure 4) and with the results of the competitive binding studies involving both calicheamicin and calicheamicin oligosaccharide (Figure 5). We cannot exclude the possibility, however, that the preactivated complex for which we have obtained binding constants is distinct from the initial complex that forms between calicheamicin and DNA.

In trying to account for the difference between our observations and predictions based on previously reported kinetic data, we are faced with two possibilities: either the dissociation rate is slower in our situation than in the NMR analysis conducted by Kahne and colleagues or the rate of thiol-dependent activation is faster in our reaction system than in the one studied by Townsend and colleagues. Arguing for the former possibility is the fact that the NMR analysis utilized an 8mer duplex DNA containing the target sequence 5′-ACCT·AGGT,[12] while we tested a 20mer containing the target sequence TCCT·AGGA. Calicheamicin may bind more weakly at ACCT sites compared to TCCT sites, this difference being due to a faster dissociation rate (see below). Arguing for the latter possibility, there are a number of differences between our reaction system and that employed by Townsend and colleagues,[15] including temperature (37 °C vs 25 °C), solvent composition (10% DMSO in H_2O vs 30% MeOH in H_2O), choice of thiol (β-mercaptoethanol vs aminoethanethiol), and target DNA (synthetic 20mer vs total calf thymus DNA).

Early reports concerning calicheamicin-induced DNA cleavage took note of the remarkable sequence specificity of the reaction—cleavage occurs preferentially at 5′-TCCT·AGGA and 5′-CTCT·AGAG sites within duplex DNA.[1] Later studies showed that other oligopyrimidine·oligopurine sites, such as 5′-TCCC·GGGA and 5′-TTTT·AAAA, could be targeted.[16] Even the rule of oligopyrimidine·oligopurine specificity can be violated by target sequences such as 5′-ACCT·AGGT. We find that calicheamicin can cleave a wide variety of target sequences, provided one supplies a sufficiently high concentration of the drug to saturate what might be a relatively unfavorable binding site. There will be a characteristic K_D value for each of these sites, with 5′-TCCT·AGGA, 5′-CTCT·AGAG, and 5′-TCCC·GGGA sites likely exhibiting the tightest binding. These sequences contain a run of pyrimidines that can be distorted to accommodate calicheamicin binding within the minor groove[12] and in addition contain a guanine residue at the appropriate position for interaction with the iodine substituent on the C ring of the oligosaccharide. It should be possible to measure DNA binding constants for other high-affinity sites just as we have done for TCCT·AGGA, but this will not be possible for low-affinity sites that are not amenable to analysis of burst kinetics.

The soil bacterium *Micromonospora echinospora calichensis* that produces the calicheamicins presumably uses these compounds to defend against viral or bacterial pathogens. Based on

(15) Chatterjee, M.; Cramer, K. D.; Townsend, C. A. *J. Am. Chem. Soc.* **1993**, *115*, 3374–3375.
(16) Walker, S.; Landovitz, R.; Ding, W. D.; Ellestad, G. A.; Kahne, D. *Proc. Natl. Acad. Sci. U.S.A.* **1992**, *89*, 4608–4612.

initial isolates from fermentation broths,[17] it is likely that the natural form of calicheamicin is either calicheamicin γ_1^{Br} or calicheamicin β_1^{Br}, both of which carry a bromo-substituted oligosaccharide. It was only after sodium iodide was added to the fermentation medium that calicheamicin γ_1^1 was obtained.[18] Considering the relative affinity of the corresponding oligosaccharides, calicheamicin γ_1^{Br} is expected to bind at TCCT·AGGA sites with somewhat lower affinity compared to calicheamicin γ_1^1. It is difficult to predict whether the bromo analogue has higher or lower sequence specificity compared to the iodinated form.

Binding of calicheamicin at TCCT·AGGA sites within duplex DNA is the result primarily of interactions involving the oligosaccharide domain, which account for 7.6 kcal mol^{-1} of the total binding energy of 9.7 kcal mol^{-1}. The difference of 2.1 kcal mol^{-1} may be attributed either to interactions involving the enediyne moiety or to interactions involving the oligosaccharide that occur only in the context of the intact molecule. Previous studies have implicated the iodine substituent as playing a critical role in DNA recognition.[10] Indeed, removal of this substituent results in the loss of 2.3 kcal mol^{-1} of binding energy when measured in the context the oligosaccharide domain alone. Other halogen substitutions have an intermediate effect (Table 1). There is a good correlation between the atomic radius of the halogen substituent and the stability of the oligosaccharide–DNA complex ($r = +0.90$), suggesting that the halogen makes a specific contact within the minor groove of the DNA.

Replacement of iodine by a methyl group, which has an atomic radius intermediate between that of iodine and bromine, results in a binding energy that is lower even than that of the chloro compound. Thus the interaction between the halogen substituent and the DNA is due not simply to van der Waals contacts but also to the chemical nature of the substituent. It has been suggested that the polarizable iodine interacts with the exocyclic C2-NH_2 of both guanine residues at the target site.[11] Based on recent NMR data[12] and the results of our inosine substitution analysis, this suggestion should be amended to focus solely on the 5′-most guanine. More recent NMR data suggest that there is a direct interaction between the iodine and the guanine C2-NH_2, which is detectable in the NOESY spectrum of the calicheamicin–DNA complex.[19]

Not all of the target sequences that are recognized by calicheamicin contain a guanine residue at the appropriate position for interaction with the iodine substituent. Furthermore, the difference in binding energy of 2.3 kcal mol^{-1} between the iodinated and deiodinated forms far exceeds what can be attributed to a single hydrogen-bonding interaction. Thus there are other specific interactions between the calicheamicin oligosaccharide and duplex DNA that need to be characterized, both structurally and kinetically. We expect that the methodology employed in this study will be useful in exploring a variety of tight-binding interactions between oligosaccharides and nucleic acids.

Experimental Section

Preparation of DNA Substrate. All DNA oligomers, purified by HPLC, were purchased from Operon Technologies (Alameda, CA) and quantitated spectrophotometrically.[20] DNA oligomers were [5′-^{32}P]-labeled in a 20-μL reaction mixture containing 20 pmol of DNA, 55 pmol of [γ-^{32}P]ATP (4.5 μCi pmol^{-1}), 10 mM $MgCl_2$, 70 mM Tris-HCl (pH 7.6), 5 mM dithiothreitol, and 20 units of T4 polynucleotide kinase, which was incubated at 37 °C for 1 h. The radiolabeled material was purified by electrophoresis in a 20% polyacrylamide/8 M urea gel and subsequent affinity chromatography on DuPont Nensorb.

DNA Cleavage Reaction. The [5′-^{32}P]-labeled, TCCT-containing DNA oligomer (1 pmol) and the unlabeled, AGGA-containing DNA oligomer (100 pmol) were hybridized in a 500-μL volume containing 100 mM NaCl and 1 mM Tris-HCl (pH 7.5), which was incubated at 95 °C for 3 min and then slow-cooled to 25 °C over 1 h. An aliquot of the hybridization mixture was added to a reaction mixture containing 20 mM NaCl, 30 mM Tris-HCl (pH 7.5), 10% DMSO (v/v), and varying concentrations of calicheamcin γ_1^1, with or without added calicheamicin oligosaccharide, in a final volume of 30 μL, which was preincubated at 37 °C for 30 min. Calicheamicin-dependent DNA cleavage was initiated by addition of 1 μL of β-mercaptoethanol (prewarmed to 37 °C) to attain a final concentration of 30 mM. Aliquots of 3 μL were taken at specified times following addition of the thiol and were transferred to dry ice-cooled Eppendorf tubes. An equal volume of gel loading buffer, containing 96% formamide, 7.5 mM Na_2EDTA, 0.05% (w/v) Bromophenol Blue, and 0.05% (w/v) xylene cyanol, was added, and the samples were stored at −70 °C.

Quantitation by Gel Electrophoresis. All samples were analyzed by electrrophoresis in a 20% polyacrylamide/8 M urea gel. Bands corresponding to both the cleaved and uncleaved [5′-^{32}P]-labeled DNA oligomers were visualized by autoradiography, cut from the gel, and quantitated by Cerenkov counting in a scintillation counter. In all cases, a correction was made for background counts based on a control lane of the gel that contained DNA that had been incubated in the absence of calicheamicin; background counts in the cleavage band were typically about 1% of total counts.

Synthesis of Calicheamicin Oligosaccharides. Oligosaccharides **2–7** were obtained by chemical synthesis according to the general scheme already reported from these laboratories.[21] The substituent on the aromatic ring was introduced at the bicyclic stage by metal exchange of the iodine atom, followed by quenching with the appropriate reagent as described below. Selected physical data for these compounds are given below.

Methyl 4,6-Dideoxy-4-[*N*-[(2,6-dideoxy-4-[*S*-[4-[(6-deoxy-3-*O*-methyl-α-L-mannopyranosyl)oxy]-3-iodo-5,6-dimethoxy-2-methylbenzoyl]thio]-β-D-*ribo*-hexopyranosyl)oxy]amino]-2-*O*-(2,4-dideoxy-4-(ethylamino)-3-*O*-methyl-α-L-*threo*-pentopyranosyl)-β-D-glucopyranoside (2). The synthesis and physical characterization of **2** were reported in ref 21.

Methyl 4,6-dideoxy-4-[*N*-[(2,6-dideoxy-4-[*S*-[4-[(6-deoxy-3-*O*-methyl-α-L-mannopyranosyl)oxy]-3-bromo-5,6-dimethoxy-2-methylbenzoyl]thio]-β-D-*ribo*-hexopyranosyl)oxy]amino]-2-*O*-(2,4-dideoxy-4-(ethylamino)-3-*O*-methyl-α-L-*threo*-pentopyranosyl)-β-D-glucopyranoside (3). The fully protected rhamnose–aryl methyl ester system was reacted with MeLi and then *N*-bromosuccinimide to give the corresponding bromo derivative, which was taken through the synthesis[21] to furnish compound **3**. **3**: R_f = 0.16 (15% MeOH in EtOAc); $[\alpha]^{23}_D$ −40° (c = 0.55, $CHCl_3$); IR ($CHCl_3$) ν_{max} 3445, 2933, 1673 cm^{-1}; ^{1}H NMR (500 MHz, $CDCl_3$) δ 6.36 (bs, 1 H, ON*H*), 5.65 (s, 1 H, D-1), 5.42 (bs, 1 H, E-1), 5.06 (dd, J = 10.1, 1.6 Hz, 1 H, B-1), 4.45 (dd, J = 4.5, 1.7 Hz, 1 H, D-2), 4.31 (bd, J = 2.5 Hz, 1 H, B-3), 4.22 (d, J = 7.8 Hz, 1 H, A-1), 4.21 (m 1 H, E-5eq), 4.07 (m, 1 H, B-5), 4.00 (t, J = 9.6 Hz, 2 H, A-3, E-3), 3.88 (s, 3 H, aromatic-OCH_3), 3.84 (s, 3 H, aromatic-OCH_3), 3.83–3.70 (m, 3 H, B-4, D-3, E-5ax), 3.66–3.57 (m, 2 H, A-5, D-4), 3.56 (s, 3 H, C*H*$_3$O-A ring), 3.53 (s, 3 H, C*H*$_3$O-D ring), 3.48 (dd, J = 8.0, 8.0 Hz, 1 H, A-2), 3.38 (s, 3 H, C*H*$_3$O-E ring), 2.73 (m, 3 H, E-4, C*H*$_2$N), 2.34 (d, J = 10.4 Hz, 1 H, A-4), 2.30 (m, 1 H, E-2eq), 2.29 (s, 3 H, C*H*$_3$-aromatic), 2.02 (bd, J = 12.9 Hz, 1 H, B-2eq), 1.78 (ddd, J = 13.0, 10.4, 2.5 Hz, 1 H, B-2ax), 1.52 (ddd, J = 13.5, 10.1, 3.5 Hz, 1 H, E-2ax), 1.41 (d, J = 6.3 Hz, 3 H, B-6), 1.34 (d, J = 6.2 Hz, 3 H, A-6), 1.30 (d, J = 6.2 Hz, 3 H, D-6), 1.17 (t, J = 7 Hz, 3 H, C*H*$_3$CH$_2$N); ^{13}C NMR (125 MHz, $CDCl_3$) δ 191.8, 149.5, 149.3, 144.4, 130.8, 130.2, 115.1, 102.6, 102.4, 99.7, 98.2, 80.9, 78.2, 76.1, 71.0, 70.2, 69.1, 68.3, 68.1, 66.8, 61.7, 61.3, 61.0, 59.1, 57.2, 56.8, 56.0, 51.6, 41.8, 36.9, 33.8, 29.7, 19.7, 18.9, 17.7, 17.6, 14.9; HRMS (FAB) calcd for $C_{38}H_{61}BrCsN_2O_{17}S$ 1061.1929, found 1061.1901.

Methyl 4,6-Dideoxy-4-[*N*-[(2,6-dideoxy-4-[*S*-[4-[(6-deoxy-3-*O*-methyl-α-L-mannopyranosyl)oxy]-3-chloro-5,6-dimethoxy-2-methylbenzoyl]thio]-β-D-*ribo*-hexopyranosyl)oxy]amino]-2-*O*-(2,4-dideoxy-4-(ethylamino)-3-*O*-methyl-α-L-*threo*-pentopyranosyl)-β-D-glucopyranoside (4). Compound

(17) Lee, M. D.; Manning, J. K.; Williams, D. R.; Kuck, N. A.; Testa, R. T.; Borders, D. B. *J. Antibiot.* **1989**, *42*, 1070–1087.
(18) Lee, M. D.; Dunne, T. S.; Chang, C. C.; Siegel, M. M.; Morton, G. O.; Ellestad, G. A.; McGahren, W. J.; Borders, D. B. *J. Am. Chem. Soc.* **1992**, *114*, 985–997.
(19) Paloma, L. G.; Smith, J. A.; Chazin, W. J.; Nicolaou, K. C. *J. Am. Chem. Soc.*, preceding paper in this issue.
(20) Cantor, C. R.; Warshaw, M. M. *Biopolymers* **1970**, *9*, 1059–1077.
(21) (a) Nicolaou, K. C.; Groneberg, R. D.; Miyazaki, T.; Stylianides, N. A.; Schulze, T. J.; Stahl, W. *J. Am. Chem. Soc.* **1990**, *112*, 8193–8195. (b) Groneberg, R. D.; Miyazaki, T.; Stylianides, N. A.; Schulze, T. J.; Stahl, W.; Schreiner, E. P.; Suzuki, T.; Iwabuchi, Y.; Smith, A. L.; Nicolaou, K. C. *J. Am. Chem. Soc.* **1993**, *115*, 7593–7611.

4 was synthesized according to the same procedures as for the preparation of **3** except for the use of carbon tetrachloride to quench the lithio derivative. **4**: R_f = 0.16 (15% MeOH in EtOAc); $[\alpha]^{23}_D$ –44° (c = 0.32, $CHCl_3$); IR ($CHCl_3$) ν_{max} 3423, 2933, 1672 cm^{-1}; ^1H NMR (500 MHz, $CDCl_3$) δ 6.36 (bs, 1 H, ONH), 5.60 (d, J = 1.5 Hz, 1 H, D-1), 5.44 (bs, 1 H, E-1), 5.05 (dd, J = 10.1, 1.8 Hz, 1 H, B-1), 4.44 (dd, J = 3.1, 1.8 Hz, 1 H, D-2), 4.31 (bd, J = 2.8 Hz, 1 H, B-3), 4.23 (d, J = 7.7 Hz, 1 H, A-1), 4.22 (m, 2 H, D-5, E-5eq), 4.09 (m, 1 H, B-5), 4.00 (t, J = 9.6 Hz, 2 H, A-3, E-3), 3.87 (s, 3 H, aromatic-OCH_3), 3.85 (s, 3 H, aromatic-OCH_3), 3.80 (dd, J = 10.4, 4.6 Hz, 1 H, E-5ax), 3.76 (dd, J = 10.8, 2.6 Hz, 1 H, B-4), 3.68 (dd, J = 9.3, 3.2 Hz, 1 H, D-3), 3.66 (dd, J = 9.7, 6.2 Hz, 1 H, A-5), 3.61 (dd, J = 9.4, 9.4 Hz, 1 H, D-4), 3.56 (s, 3 H, CH_3O-A ring), 3.55 (s, 3 H, CH_3O-D ring), 3.46 (dd, J = 9.2, 7.9 Hz, 1 H, A-2), 3.40 (s, 3 H, CH_3O-E ring), 2.95, 2.82 (bm, 2 H, CH_2N), 2.81 (m, 1 H, E-4), 2.38 (ddd, J = 13.0, 4.7, 2.9 Hz, 1 H, E-2eq), 2.34 (dd, J = 9.7, 9.7 Hz, 1 H, A-4), 2.25 (s, 3 H, CH_3-aromatic), 2.03 (dt, J = 13.4, 3.6 Hz, 1 H, B-2eq), 1.79 (ddd, J = 13.3, 10.5, 2.8 Hz, 1 H, B-2ax), 1.52 (ddd, J = 13.3, 9.9, 3.5 Hz, 1 H, E-2ax), 1.41 (d, J = 6.2 Hz, 3 H, B-6), 1.34 (d, J = 6.2 Hz, 3 H, A-6), 1.30 (d, J = 6.3 Hz, 3 H, D-6), 1.24 (obs, 3 H, CH_3CH_2N); ^{13}C NMR (125 MHz, $CDCl_3$) δ 191.8, 148.8, 148.3, 144.8, 130.8, 128.6, 123.8, 102.7, 102.4, 99.8, 97.8, 80.9, 78.3, 71.1, 70.9, 70.6, 70.0, 69.1, 68.4, 68.3, 68.1, 66.8, 61.8, 61.0, 58.2, 57.2, 56.1, 51.6, 41.9, 36.9, 33.7, 29.7, 19.0, 17.7, 17.6, 16.6; HRMS (FAB) calcd for $C_{38}H_{61}ClCsN_2O_{17}S$ 1017.2434, found 1017.2444.

Methyl 4,6-Dideoxy-4-[*N*-[(2,6-dideoxy-4-[*S*-[4-[(6-deoxy-3-*O*-methyl-α-L-mannopyranosyl)oxy]-5,6-dimethoxy-3-fluoro-2-methylbenzoyl]thio]-β-D-*ribo*-hexopyranosyl)oxy]amino]-2-*O*-(2,4-dideoxy-4-(ethylamino)-3-*O*-methyl-α-L-*threo*-pentopyranosyl)-β-D-glucopyranoside (5). Compound **5** was synthesized according to the same procedures described for **3** except for the use of *N*-fluorobis(phenylsulfonyl)amine to introduce the fluorine atom. **5**: R_f = 0.16 (15% MeOH in EtOAc); $[\alpha]^{20}_D$ –48° (c = 0.13, $CHCl_3$); IR (neat) ν_{max} 3414, 2928, 1674, 1462, 1358, 1112, 1066, 1024, 984, 929, 802, 756, 613, 506 cm^{-1}; ^1H NMR (500 MHz, $CDCl_3$) δ 6.31 (bs, 1 H, ONH), 5.52 (bd, J = 1.5 Hz, 1 H, D-1), 5.43 (dd, $J \approx$ 3.2, 1.4 Hz, 1 H, E-1), 5.05 (dd, J = 10.2, 2.0 Hz, 1 H, B-1), 4.41 (dd, $J \approx$ 2.5, 1.5 Hz, 1 H, D-2), 4.32 (m, 1 H, B-3), 4.23 (d, J = 7.7 Hz, 1 H, A-1), 4.17 (m, 1 H, D-5), 4.08 (dq, J = 10.8, 6.2 Hz, 1 H, B-5), 4.00 (t, J = 9.6 Hz, 1 H, A-3), 3.88 (s, 3 H, aromatic-OCH_3), 3.87 (obs, 1 H, E-5), 3.85 (s, 3 H, aromatic-OCH_3), 3.77 (dd, J = 10.8, 2.7 Hz, 1 H, B-4), 3.74 (m, 1 H, E-5′), 3.65 (dq, J = 9.6, 6.2 Hz, 1 H, A-5), 3.64–3.61 (m, 2 H, D-3, D-3), 3.62 (obs, 1 H, E-3), 3.55 (s, 3 H, CH_3O-A ring), 3.54 (s, 3 H, CH_3O-D ring), 3.48 (dd, J = 9.2, 7.8 Hz, 1 H, A-2), 3.39 (s, 3 H, CH_3O-E ring), 2.82–2.64 (m, 3 H, CH_2N, E-4), 2.34 (t, J = 9.7 Hz, 1 H, A-4), 2.33 (m, 1 H, E-2eq), 2.15 (d, $^4J_{F,H}$ = 2.3 Hz, 3 H, CH_3-aromatic), 2.03 (m, 1 H, B-2eq), 1.78 (m, 1 H, B-2ax), 1.53 (m, 1 H, E-2ax), 1.41 (d, J = 6.2 Hz, 3 H, B-6), 1.34 (d, J = 6.2 Hz, 3 H, A-6), 1.31 (d, J = 6.2 Hz, D-6), 1.18 (m, 3 H, CH_3CH_2N); ^{19}F NMR (377 MHz, $CDCl_3$, internal standard $CFCl_3$) δ –135.9; ^{13}C NMR (125 MHz, $CDCl_3$) δ 191.2, 150.7 (d, $^1J_{F,C}$ = 244 Hz), 146.1, 145.0, 130.0, 117.5 (d, $^2J_{F,C}$ = 22 Hz), 102.7, 102.1, 99.7, 98.5, 80.9, 78.2, 76.9, 71.09, 71.04, 69.6, 69.0, 68.4, 68.3, 68.2, 66.7, 62.2, 62.0, 61.2, 59.4, 57.2, 56.8, 51.6, 41.9, 36.8, 33.9, 29.7, 18.9, 17.7, 17.5, 15.6, 13.7; HRMS (FAB) calcd for $C_{38}H_{61}FN_2O_{17}S + Cs^+$ 1001.2729, found 1001.2681.

Methyl 4,6-Dideoxy-4-[*N*-[(2,6-dideoxy-4-[*S*-[4-[(6-deoxy-3-*O*-methyl-α-L-mannopyranosyl)oxy]-5,6-dimethoxy-2,3-dimethylbenzoyl]thio]-β-D-*ribo*-hexopyranosyl)oxy]amino]-2-*O*-(2,4-dideoxy-4-(ethylamino)-3-*O*-methyl-α-L-*threo*-pentopyranosyl)-β-D-glucopyranoside (6). Compound **6** was synthesized according to the same procedures described for **3** except for the use of methyl triflate to introduce the methyl group. **6**: R_f = 0.16 (15% MeOH in EtOAc); $[\alpha]^{20}_D$ –39° (c = 0.4, $CHCl_3$); IR (neat) ν_{max} 3430, 2928, 1672, 1488, 1460, 1064 cm^{-1}; ^1H NMR (500 MHz, $CDCl_3$) δ 6.32 (bs, 1 H, ONH), 5.43 (dd, $J \approx$ 3.2, 1.4 Hz, 1 H, E-1), 5.38 (d, J = 1.5 Hz, 1 H, D-1), 5.04 (dd, J = 10.2, 1.7 Hz, 1 H, B-1), 4.43 (bs, 1 H, D-2), 4.31 (m, 1 H, B-3), 4.22 (d, J = 7.7 Hz, 1 H, A-1), 4.11 (m, 1 H, D-5), 4.08 (dq, $J \approx$ 11, 6.2 Hz, 1 H, B-5), 4.00 (t, J = 9.5 Hz, 1 H, A-3), 3.85 (s, 3 H, aromatic-OCH_3), 3.84 (obs, 1 H, E-5), 3.83 (s, 3 H, aromatic-OCH_3), 3.75 (dd, J = 10.9, 2.5 Hz, 1 H, B-4), 3.72 (dd, J = 11.2, 4.8 Hz, 1 H, E-5′), 3.65 (dq, J = 9.6, 6.2 Hz, 1 H, A-5), 3.62 (m, 2 H, D-3, D-4), 3.56 (s, 3 H, CH_3O), 3.54 (obs, 1 H, E-3), 3.53 (s, 3 H, CH_3O), 3.49 (dd, J = 9.3, 7.7 Hz, 1 H, A-2), 3.38 (s, 3 H, CH_3O), 2.77–2.62 (m, 2 H, CH_2N), 2.71 (m, 1 H, E-4), 2.33 (t, J = 9.7 Hz, 1 H, A-4), 2.33 (m, 1 H, E-2eq), 2.15 (s, 3 H, CH_3-aromatic), 2.12 (s, 3 H, CH_3-aromatic), 2.02 (m, 1 H, B-2eq), 1.77 (m, 1 H, B-2ax), 1.53 (m, 1 H, E-2ax), 1.42 (d, J = 6.2 Hz, 3 H, B-6), 1.34 (d, J = 6.2 Hz, 3 H, A-6), 1.33 (d, J = 6.2 Hz, 3 H, D-6), 1.15 (t, J = 7.1 Hz, 3 H, CH_3-CH_2N); ^{13}C NMR (125 MHz, $CDCl_3$) δ 193.0, 150.6, 147.8, 143.5, 130.6, 128.6, 126.6, 102.9, 102.7, 99.7, 98.3, 81.2, 78.2, 76.4, 71.09, 71.07, 69.8, 69.0, 68.3, 68.2, 67.0, 61.7, 60.8, 59.2, 57.1, 56.8, 51.6, 41.9, 36.7, 33.8, 29.7, 19.0, 17.67, 17.64, 16.1, 15.2, 12.9; HRMS (FAB) calcd for $C_{39}H_{64}N_2O_{17}S + Cs^+$ 997.2980, found 997.2991.

Methyl 4,6-Dideoxy-4-[*N*-[(2,6-dideoxy-4-[*S*-[4-[(6-deoxy-3-*O*-methyl-α-L-mannopyranosyl)oxy]-5,6-dimethoxy-2-methylbenzoyl]thio]-β-D-*ribo*-hexopyranosyl)oxy]amino]-2-*O*-(2,4-dideoxy-4-(ethylamino)-3-*O*-methyl-α-L-*threo*-pentopyranosyl)-β-D-glucopyranoside (7). Compound **7** was obtained by reducing **2** with lithium aluminum hydride (THF, –78 °C). The synthesis and physical characterization of **7** were reported in ref 21.

Acknowledgment. We thank Gary Siuzdak and Dee H. Huang for assistance with mass spectroscopy and NMR spectroscopy, respectively. This work was supported by the National Institutes of Health and The Scripps Research Institute.